NC STATE UNIVERSITY

JTATM

JOURNAL OF TEXTILE AND APPAREL, TECHNOLOGY AND MANAGEMENT

Volume 1, Issue 1, September 2000

FORMATION OF SHAPED/MOLDED MELTBLOWING NONWOVEN STRUCTURES

Yogeshwar Velu, Raoul Farer, Tushar Ghosh, Abdelfattah Seyam
North Carolina State University

ABSTRACT

Three dimensional (3D) fiberweb structures are useful in many applications. The Robotic Fiber Assembly and Control System (RFACS) being developed in this research allows precise control of fiber meltblown fiber deposition on a 3D mold surface. The effect of various process parameters on a number of polypropylene (PP) web characteristics is reported. Under the experimental range studied, the fiber orientation distribution was significantly impacted by the process parameters. The fiber diameter distributions indicate that they are unique to a particular process condition. The distributions do not overlap when a parameter is evaluated. In keeping with the long-term objective of developing chemical/biological barrier fabrics using RFACS technology, the pore distribution of the fiberwebs was characterized. Under the conditions explored, the average pore size of the analyzing web has decreased by 60% when the attenuating air pressure was increased from 0.7 bar to 2.8 bar. The pore size was decreased by 33% when the take up speed of the web was increased from 20 ft/min to 50 ft/min.

1. INTRODUCTION

Nonwoven webs can be produced as sheet structures by using meltblown technology [23]. In meltblowing, molten polymer is extruded through a series of orifices in a knife-edge die. The die is jacketed on both sides by high velocity laminar sheets of air. The polymer streams from the orifices are elongated by the air-drag to form fibers, which are collected on a drum or other suitable collecting surface. Fiber diameters can range from 500 microns to as small as 0.1 microns (μm). The extreme entanglement of fibers, characterizing meltblown fibrous webs, produces coherency and strength. The density of the web is such that it has the property to contain and retain particulate matter [12], thus qualifying such structures for filtration applications. The entanglement of these long fibers makes it impossible to remove one fiber from the web or to trace one fiber from beginning to end [7]. Meltblown webs are lightweight with a high surface area. They display a high insulating value and excellent filter characteristics [3, 17]. Meltblown technology can be used to produce efficient filter materials, filtering particles that are bigger than 0.5 μm [24].

The long term objective of this research is to develop technology to produce shaped protective garments, substantially to its final shape and using minimal seaming or joining. The latter usually constitute the "weak-link" in a protective system. The integration of meltblowing technology and robotics can achieve the proper formation of molded or shaped seamless structure that may be incorporated in a protective clothing system. In integrating the two technologies the fiber web collector is usually a mold object structure. The mold can be manipulated to rotate continuously so as to form the molded fabric. The size of the die width should be smaller than the size of the mold to have a good control over the deposition of the fibers on the mold.

The usefulness of molded fabrics so obtained depends on the performance characteristics of the web structures. The desired performance characteristics, globally and locally, can be enumerated as strength, abrasion resistance, tear

resistance, burst strength, elastic recovery, air/moisture permeability, moisture/fluid absorption (rate and capacity), filtration characteristics, etc. Each of these characteristics is influenced by fiber diameter and its distribution, pore size and its distribution, fiber orientation, web consolidation (thickness, bonding), web basis-weight (local), fiber/polymer properties, etc.

The web structure defined by fiber Orientation Distribution Function (ODF) governs the anisotropy of mechanical (strength, tear resistance, bending rigidity, etc.) and physical (wicking/absorption, pore shapes, pore size distribution, etc.) properties [9-11, 13-15]. ODF data for meltblown webs has not been available in the literature previously, while some published ODF results for spunbonded fabrics are generally similar to those found for meltblown webs in this study.

Although meltblowing process produces finer fibers relative to conventional fiber spinning processes, the distributions of fiber diameter are usually quite broad. Because lower mean values and narrower distributions lead to smaller pore sizes (lower mean and narrow distributions) and higher specific surface, the control of fiber diameter distribution is considered highly desirable [18], for a number of important applications. The pore size and its distribution in a fabric structure are of prime importance in determining the transport properties of the fabric. The filtration efficiency, and hence the level of protection, is directly related to the pore size distribution. Image Analysis techniques have been developed to measure the pore size, shape, and orientation of the pores [23, 26]. Most of the methods developed at the Textile Research Institute (TRI) use fluid intrusion or extrusion on a sample to determine the average pore size and its distribution.

2. ROBOTIC FIBER ASSEMBLY AND CONTROL SYSTEM

To produce the seamless 3D garments a Robotic Fiber Assembly and Control System (RFACS) has been set up. The RFACS consists of a model meltblown machine and a commercial six-axis robot that is capable of manipulating the meltblown die in the range of positions and orientations required for use with the complex 3D shape molds. Accurate robot positioning is required to keep the distance between the die and the mold at will while maintaining appropriate orientations with the mold. In addition, to achieve the required level of mold control needed for this process, an external seventh axis has been added. The RFACS setup is shown in Figure 1.

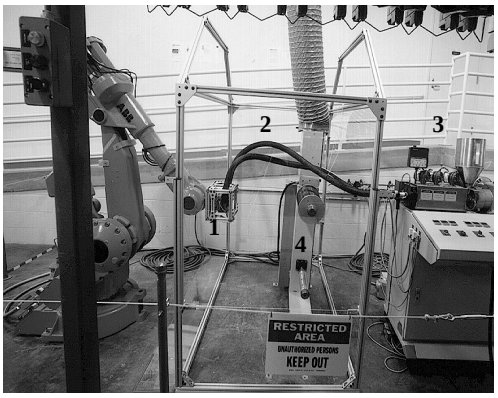

Figure 1. Robotic Fiber Assembly and Control System (RFACS)
1. Melt-Blowing Die Housed in a Cage.
2. Polymer and Air Flexible Supply Hoses.
3. Melt-Blowing Extruder Unit. 4. Collector.

The shaped nonwoven structures are produced by depositing meltblown fibers on a collapsible mold that is placed on the seventh axis of the robot. To develop the contour-following algorithms for mold shapes point coordinates on the mold shape were determined at regular rotational increments. To find these points in 3D-space for the 2D model, a pointer has been constructed such that the pointer tip assumes the virtual position of the right most orifice in the meltblowing die body. For the 3D model, a pointer mirroring the position of the polymer orifices has been constructed. The pointer uses to mark points on a mold relative to the world coordinate system. This procedure has been adopted as the means of developing the position and speed of the meltblowing die to the rotation of the mold body.

3. EFFECT OF PROCESS PARAMETERS ON WEB CHARACTERISTICS

The research documented in this paper deals with mold structures being coated with a meltblown web, hence, experiments were conducted to develop appropriate control algorithms. These algorithms would control the RFACS in a way to precisely control fiber dispensation on to the mold surface. The objective of the control algorithms is not necessarily to control uniformity of web characteristics, but to control

these locally. The web characteristics of interest in the context of the present research are (1) Basis weight, (2) Fiber orientation distribution, (3) Fiber diameter distribution, and (4) Pore size distribution. These characteristics determine the local physical, mechanical and fluid flow behavior of the web. The relevant process parameters are:

- Polymer throughput
- Die / Melt / Attenuating air temperature
- Attenuating air pressure,
- Fiber stream approach angle,
- Take-up speed, and
- Relative orientation and movement of die

In the following, the parametric studies are reported and categorized according to their influence on a specific web characteristics.

Basis Weight

The basis weight (g/m^2) of the PP fabric was evaluated by measuring the weight of known area of fabric samples at regular intervals, along the surface of the mold. The variation in measured basis weight is expressed as percent coefficient of variation (%CV). Initial experiments were conducted such that the die was moving up and down the mold, while the mold was rotating on the 7^{th} axis at a uniform speed (2D no correction Model). The 2D model was modified to correct for variations in the die to collector distance (DCD correction) and the linear speeds of the mold on the 7^{th} axis (linear rotational speed correction model).

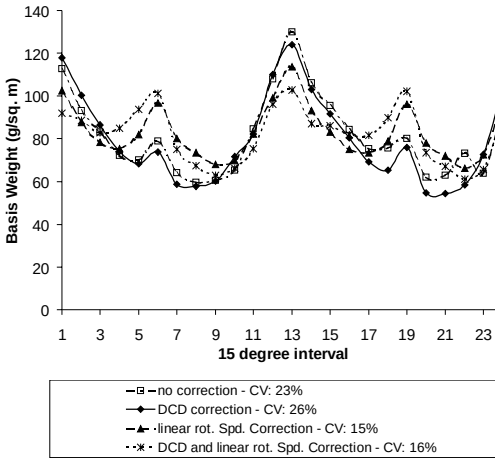

Figure 2. Two-Layer Basis-Weight Distribution Using the 2D Model

Figures 2 and 3 show the basis weight distributions using the patterns of motion variation for the 2D model. The differences in

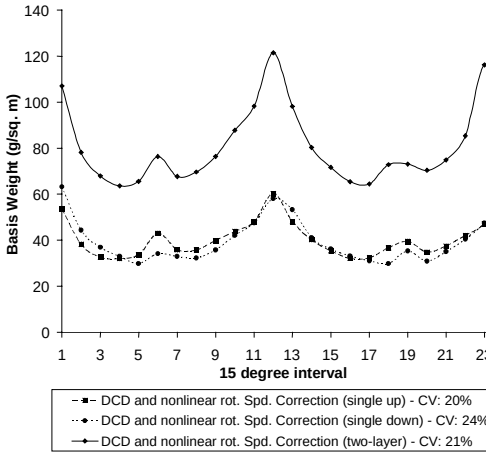

Figure 3. Single-Layer/Two-layer Basis-Weight Distribution using the 2D Model and Nonlinear Rotation Speeds

basis weight distributions are related to the interaction between the geometrical features of the mold and the characteristics of the fiber flaring profile and the die orientation. CV values for samples formed using the no correction model were 8% higher than CV values for samples obtained using the linear correction model. The difficulty in achieving more uniform basis weight distribution is inherently related to

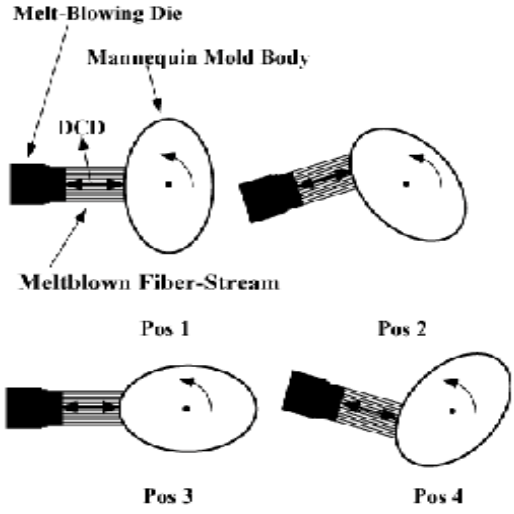

Figure 4. 3D Positioning Sequence

the die orientation during the production. When the die is not reoriented in relation to the surface of the mold during fiber application, overshot of fibers occurs. This causes loss of control for the deposition of fibers on the mold.

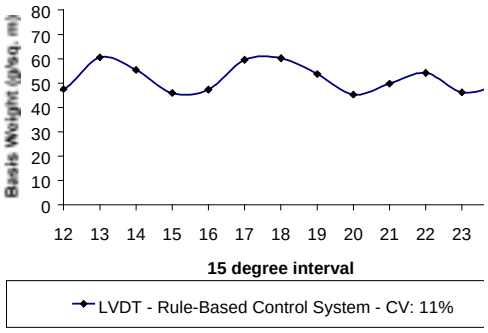

Figure 5. Rule-Based Control Results Using LVDT Feedback and 3D Triangularization

The 3D model was developed by the implementation of 3D-triangulation positioning and feedback control of the mold positioning data using the LVDT. This included the control of the movement of the die and the rotational speed of the mold mounted on the 7th axis (Figure 4). The position of the die is controlled such that the fiber streams are normal to the surface of the mold at the point of deposition of the fiber. A LVDT feed back control was used to control the speed of the 7th axis, such that the linear speed of the mold surface was constant. The overall control performance improved with the use of the 3D model [7]. Using the rule-based control resulted in the lowest overall CV values (11%) for basis-weight uniformity as it can be seen from the results of Figure 5. Since previous experimentation had shown basis weight effects to be symmetric around 180 degrees, only one side of the mold was evaluated.

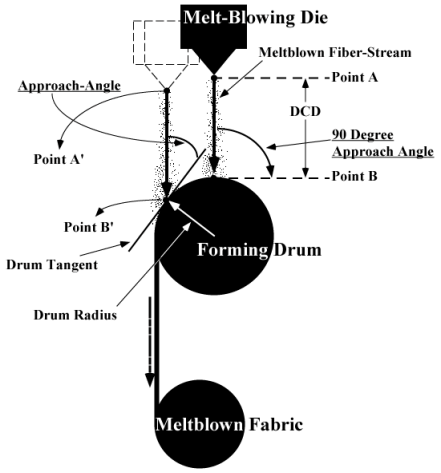

Figure 2. Fiber-Stream Approach-Angle

Fiber Orientation Distribution

The orientation distribution function (ODF) of the fibers was measured on samples that were prepared using the 90° fiber approach angle (Figure 6) relative to the collector drum. An image analysis package developed at the Nonwovens Cooperative Research Center was used to make ODF measurements on the samples. Influence of various process parameters on fiber orientation distribution is discussed below.

Take-Up Speed

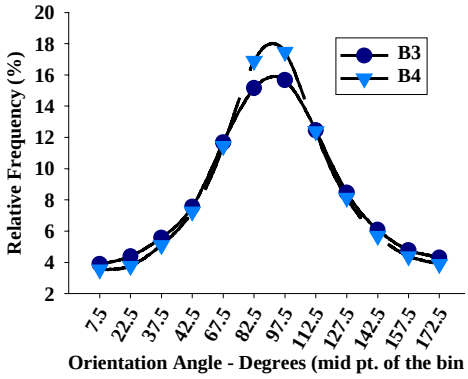

Figure 7. ODF for MB PP fabrics at different take-up speeds; 7 x 10^{-2} g/min/hole polymer throughput rate; 1.4 bar attenuating air pressure; 14 cm DCD and 282 ºC air temp. ; B3: 18 m/min and B4: 24 m/min.

Figure 7 gives the ODF for fabrics formed at take-up speeds of 18, and 24 m/min, while other process parameters are held constant. Note that with extruder output kept constant the basis weight decreases with increasing take-up speed. The results show an increase in orientation with an increase in take-up speeds.

Maximum observed fiber fraction data along the machine direction (MD) in Figure 8, depicts increases in orientation along MD with increases in take-up speeds for all fabric types evaluated. Webs do not initially exhibit significant changes in its ODF at take-up speeds below 18.3 m/min. This may be due to aerodynamic interaction with

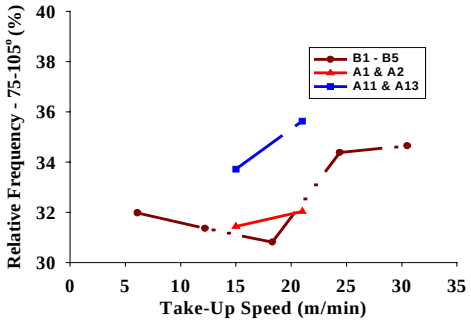

Figure 8. Maximum observed fiber fraction along "MD" for MB PP fabrics at different take-up speeds; 282 ºC air temp.; B1-B5: 7 x 10^{-2} g/min/hole polymer throughput rate, 1.4 bar attenuating air pressure, and 14 cm DCD; A1 & A2: 5.4 x 10^{-2} g/min/hole polymer throughput rate, 1.4 bar attenuating air pressure, and 14 cm DCD; Ap11 & Ap13: 5.4 x 10^{-2} g/min/hole polymer throughput rate, 0.7 bar attenuating air-pressure, and 18 cm DCD.

fibers. For take-up speeds above 18.3 m/min fabrics show higher orientation due to higher drum surface velocity induced fiber alignment along the machine direction.

Die-to-Collector-Distance (DCD)

Figure 9 shows the ODF for fabrics formed at DCD settings ranging from 14 to 31 cm. Fiber orientation is shown to continuously increase from DCD settings 31 to 14 cm. All webs evaluated are shown to exhibit less MD orientation when formed at larger DCD settings. With longer distances the turbulent fiber flow, undulating, or flapping motion of the fibers is known to increase [6, 16]. As the air velocity reduces at longer distances from the die, and loses some of its initial planar characteristics, the air volume disturbed and the dimensions of the air stream increase [18, 19]. With higher freedom of movement, and lower fiber velocity the fibers appear to take on a more random orientation in the air stream. This effect subsequently translates to reduced MD orientation in webs formed, upon collection at larger distances (higher DCD settings) from the die body.

At a DCD setting of 7 cm, webs exhibited reduced "MD" orientation relative to those formed at 14 cm. This effect is attributed to some fibers being unable to successfully develop a forward flow pattern below DCD settings of 14 cm, and rapid successive, more random, accumulation of short segments of fiber on top of each other. Some fibers are suspected to be essentially blown into themselves, thereby causing less overall orientation in the structures formed. It is also stipulated that air velocities are still much higher at small DCD values, thus bouncing back from the forming drum and thereby disturbing the MD orientation of fibers.

Fiber-Stream Approach-Angle

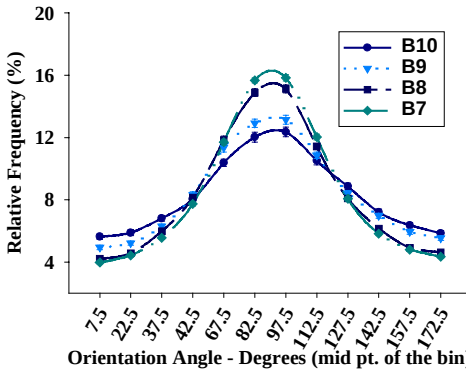

Figure 9. ODF for MB PP fabrics at different DCD; 7 x 10^{-2} g/min/hole polymer throughput rate, 1.4 bar attenuating air pressure, 21 m/min take-up speed, and 282 ºC air temp.; B7: 14 cm; B8: 21 cm; B9: 26 cm; and B10: 31 cm.

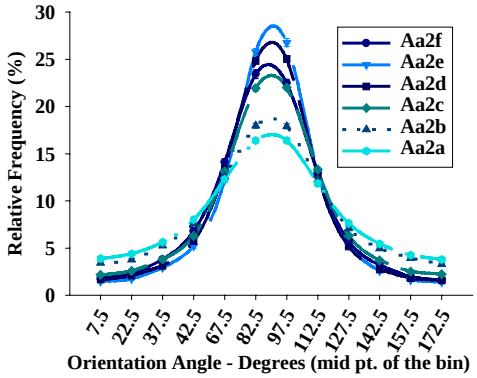

Figure 10. ODF for MB PP fabrics at different fiber-stream approach-angles; 5.4 x 10^{-2} g/min/hole polymer throughput rate, 1.4 bar attenuating air pressure, 21 m/min take-up speed, 14 cm DCD, and air temp. 305 ºC; Aa2a: 90º; Aa2b: 79º; Aa2c: 61º; Aa2d: 46º; Aa2e: 36º; and Aa2e: 26 .

Figure 10, shows the fiber ODF for fabrics formed at approach-angles ranging from 90° to 26°. Fiber fraction along MD is shown to increase by 60 % when the fiber-stream approach-angle changes from normal to 36 °. A 0 ° approach-angle would identify a fiber-stream path parallel to the tangent of the fiber forming-drum (essentially blowing past it). By reducing the fiber-stream approach-angle, some fibers will travel a longer path before being collected on the drum's surface (see Figure 4). Those fibers, which travel a longer path, are also traveling at a path more parallel to the tangent of the forming-drum, and exhibit this orientation upon collection. This effect contributes to an increase in orientation in the machine direction. This pattern continues up to a point where some fibers are actually blowing past the drum, but are pulled back into the fabric because their fiber ends are anchored inside the fiber stream. This effect was visually observed when collecting samples at approach-angles of 26 °. Fibers were observed blowing past the drum's surface, but due to their continuous nature were still trapped inside of the fiber stream. This either caused them to stick out of the formed fabric, or to be pulled back into it. In either case the structure of the formed fabric was disrupted, which can be observed in the data shown by the respective decrease in fiber orientation at approach-angles of 26 °.

PolymerThroughput Rate

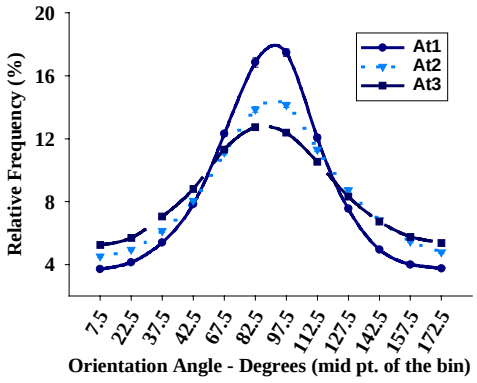

Figure 11. ODF for MB PP fabrics at different polymer throughput rate; 2.1 bar attenuating air pressure, 15 m/min take-up speed, 18 cm DCD, and 282 ºC air temp.; At1: 5.4 x 10^{-2} g/min/hole, At2: 8.1 x 10^{-2}g/min/hole, and At3: 9.6 x 10^{-2} g/min/hole.

Fiber fraction along MD decreases with increasing throughput rate, as is shown in Figure 11. In meltblowing, analogous to what occurs in melt-spinning, higher polymer throughput rate is equated with larger average fiber diameter, keeping all other conditions constant [2]. When this is the case, larger size fibers present in the fiber stream will resist aligning themselves substantially in the air flow direction and assume a more random orientation. These fibers undulate more slowly (at lower frequencies) [16], as it becomes more difficult for a thicker and heavier structure to change direction as quickly as a smaller diameter structure. Lower undulating frequencies are shown to directly result in formation of more isotropic structures.

Attenuating Air Pressure

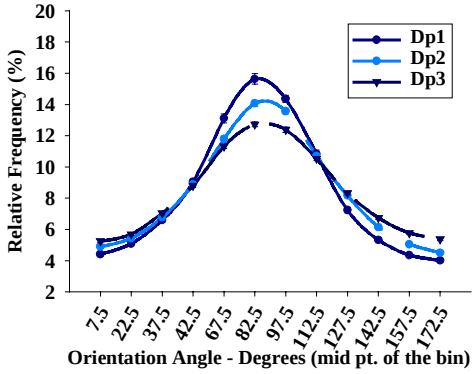

Figure 12. ODF for MB PP fabrics at different attenuating air pressures; 9.6 x 10^{-2} g/min/hole polymer throughput rate, 15 m/min take-up speed, 18 cm DCD, and 282 ºC air temp.; Dp1: 0.7 bar; Dp2: 1.4 bar, and Dp3: 2.1 bar.

Figure 12 shows ODF results from fabrics formed by varying attenuating air pressure. Fabrics are shown to be less oriented along "MD" when higher attenuating air pressures are used. If one considers that higher take-up speeds have been shown to cause more orientation, the same argument can be made here. At lower attenuating air pressures the fiber speed reduces as compared to fiber formed at higher attenuating air pressures [25]. The ratio of take-up speed to fiber speed will increase with lower attenuating air-pressures. Subsequently an argument can be made that a decrease in fiber speed, i.e. lower

attenuating air-pressure, has the same effect as an increase in take-up speed, thereby causing higher orientation to form in the fabric structure.

Fiber Diameter Distribution

SEM images at 600X were used to make the FDD measurements. Each image contained at least 20 fiber images. A well developed protocol on the image analysis software was used for adjusting the SEM image [8]. The resulting black and white fiber image was evaluated for fiber diameter. Influence of various process parameters on fiber diameter distribution is discussed below.

Polymer Throughput Rate and Attenuating Air Pressure

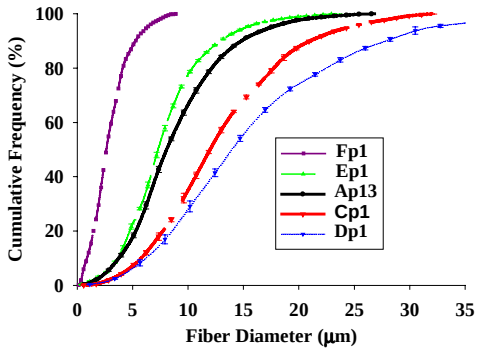

Figure 13. Cumulative frequency distribution of fiber diameters at different polymer throughput rates; 0.7 bar air pressure, 282 ºC air temp., and 260 ºC die temp.; Fp1: 1.7 x 10^{-2} g/min hole; Ep1: 3.7 x 10^{-2} g/min/hole; Ap13: 5.4 x 10^{-2} g/min/hole; Cp1: 8.1 x 10^{-2} g/min/hole; and Dp1: 9.6 x 10^{-2} g/min/hole.

Figure 13 shows cumulative frequencies of fiber diameter distributions of PP meltblown fabrics formed at different levels of polymer throughput rates and at a selected level of attenuating air pressure. Figure 14 shows cumulative frequencies of fiber diameters in fabrics produced at varying attenuating air pressure and a selected polymer throughput rate.

All web samples in Figure 13 show fiber diameters to decrease and their distribution to narrow with a decrease in throughput rate. Figure 14 shows cumulative frequencies for fiber diameter distributions in fabrics formed at varying attenuating air pressures, but a constant polymer throughput rate of 9.6 x 10^{-2} g/min/hole, and the same temperature settings as in Figure 13. Fiber diameters decrease with increase in attenuating air pressures in all cases; broader distributions of fiber diameters are observed with decreases in attenuating air pressures. All samples depict the same trend of increasing fraction of small diameter fibers with decreasing throughput rates; the increase in attenuating air

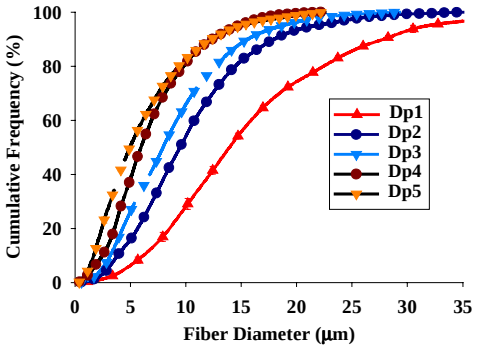

Figure 14. . Cumulative frequency distribution of fiber diameters at different attenuating air pressure; 9.6 x 10^{-2} g/min/hole throughput rate, 282 ºC air temp., and 260 ºC die temp.; Dp1: 0.7 bar; Dp2: 1.4 bar; Dp3: 2.1 bar; Dp4: 2.8 bar; and Dp5: 3.5 bar.

pressure also increases the fraction of fine (less than 10 µm) fibers. An increase in attenuating air pressure results in higher velocity of forming air, exerting higher drag forces on the polymer mass as it is being pushed out of the die orifices, as well as resulting in higher fiber velocities [2, 20]. Higher drag apparently attenuates the polymer mass to finer diameters, analogous to higher take-up roller speeds resulting in finer diameter filaments in conventional spinning.

Attenuating Air Temperature

Figure 15 shows cumulative frequencies for fiber diameter distributions obtained using varying attenuating air temperature. Fiber diameter was hardly affected by the attenuating air temperature in the range of (282 ºC – 327 ºC) studied. Similar trends were observed in a study by Rao and Shambaugh, where a 100^{0} C increase in air temperature did not show much effect on fiber diameter [16]. In both Rao and Shambaugh and our case discussed, the polymer temperature (die temperature) settings were lower than the attenuating air temperature. The air temperature measured at the die orifice does not change significantly even when the employed die

temperature is lower than the air temperature. It is observed that the attenuating air temperatures studied in this research were not high enough to cause significant changes in diameters of the fibers.

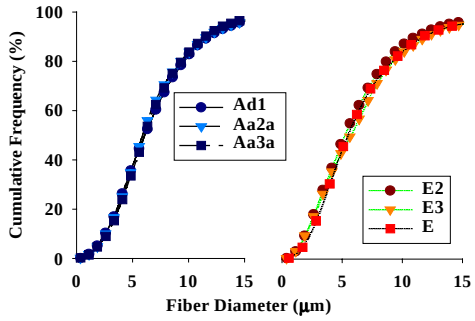

Figure 15. Cumulative frequency distribution of fiber diameters at different attenuating air temperatures; 5.4 x 10^{-2} g/min/hole throughput rate, 1.4 bar attenuating air pressure, and 260 ºC die temp.: Ad1: 282 ºC, Aa2a: 305 ºC, and Aa3a: 327 ºC; 3.7 x 10^{-2} g/min/hole throughput rate, 1.4 bar attenuating air pressure, and 260 ºC die temp.: E: 282 ºC, E2: 304 ºC, and E3: 327 ºC.

Die Temperature

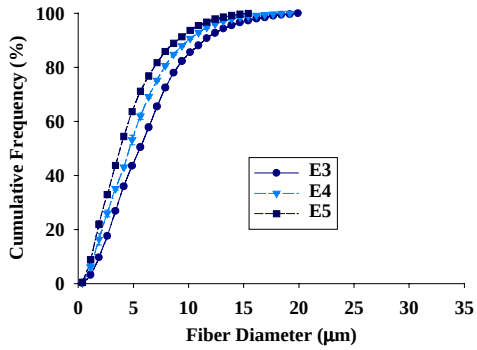

Figure 16. Cumulative frequency distribution of fiber diameters at different die temperature; 9.6 x 10^{-2} g/min/hole polymer throughput rate; 1.4 bar attenuating air pressure, and 327 ºC attenuating air temp.; E3: 260 ºC; E4: 293 ºC; and E5: 327 ºC die temperature.

Figure 16 shows cumulative frequencies for fiber diameter distributions of PP meltblown fabrics formed due to varying die temperatures. As is apparent, fiber diameter decreased with increases in die temperature. All samples show increases in fine fiber content with increasing die temperature.

The dominant resultant effect of an increase in die temperature is lower polymer viscosity in the die body. A lower viscosity liquid will show less physical resistance to high velocity attenuating air, and allow finer fiber diameters to form. The reduction in polymer viscosity appears to be more significant over the temperature range evaluated, as similar changes in air temperatures have in this study not been able to show a lasting affect. Reduction in polymer viscosity would further show a larger effect at higher polymer throughput rates, where finer diameter fibers are formed with more difficulty.

Pore Size Distribution

The pore size distribution was measured using an automated perm porometer designed and sold by the Porous Materials Inc. This equipment works on the principle of capillary flow. Details regarding the theory and the working principle of the instrument are found else where [8, 22]. Influence of various process parameters on pore size distribution is discussed below.

Die to Collector Distance

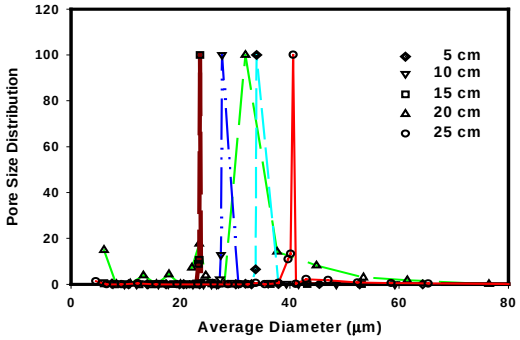

(a)

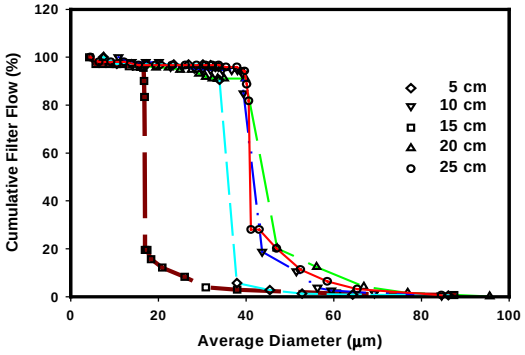

(b)

Figures 17 a & b. Pore Size Distribution and Cumulative Filter Flow (%) for MB PP Fabrics at different Die to Collector Distances. (Throughput : 3.7 x 10^{-2} g/min/hole, Air Pressure: 1.4 bar, Number of Layers: 2, Take Up Speed: 20 '/min)

Figure 17 shows normalized pore size distribution and cumulative filter flow of PP meltblown fibers formed due to varying die to collector distances. The pore size initially decreases with increase in the distance. The diameter of the pore at 15 cm is 18 microns. At this distance the web has a filtration efficiency greater than 95%, and hence particles larger than 18 microns can be filtered. Further increase in the distance of the collector, increases the diameter of the pore. An increase in die to collector distance decreases the air velocity, alters the planar nature of the air, and the temperature of the air profile. It leads to the formation of shots and hence an increase in the pore size of the web.

Number of Layers

The Pore size distribution and the cumulative filter flow for the influence of the number of layers are given in Figure 18. These graphs indicate that with increase in the number of layers the pore size decreases and the filtration efficiency increases. The technique adopted measures the smallest diameter of a given pore and thereby if a layer of fibers with relatively small pore size distribution is incorporated in the web, the overall pore size becomes smaller. With the decrease in the average pore size, the filtration efficiency increases. The data further indicates that increase in the number of layers from three to four does not have a significant effect on the pore size distribution and the filtration efficiency.

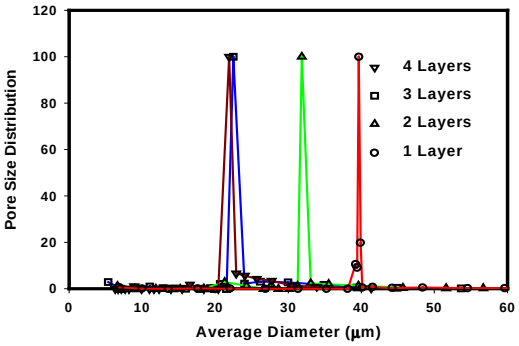

(a)

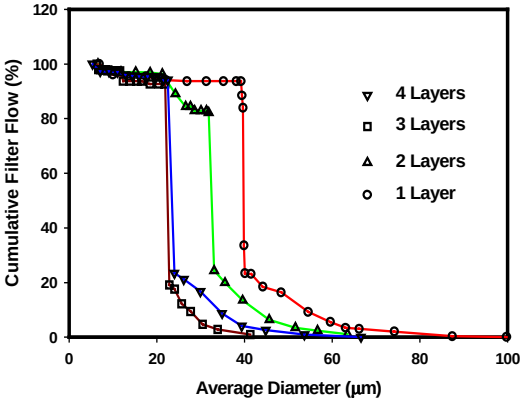

(b)

Figures 18 a & b. Pore Size Distribution and Cumulative Filter Flow (%) for MB PP Fabrics for variation in the number of layers. (Throughput : 3.7 x 10^{-2} g/min/hole, Air Pressure: 1.4 bar, DCD 15 cm, Take Up Speed: 20 '/min)

Attenuating Air Pressure

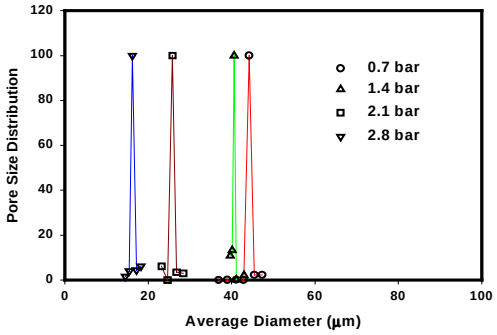

(a)

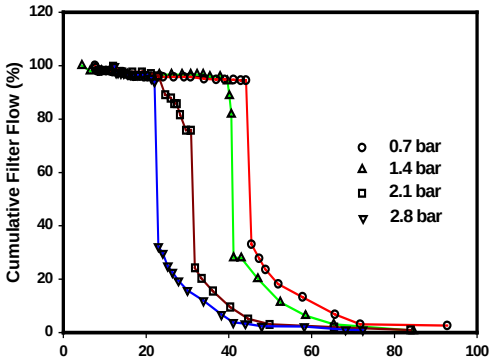

(b)

Figures 19 a & b. Pore Size Distribution and Cumulative Filter Flow(%) for MB PP Fabrics for variation in the attenuating air pressure. (Throughput : 3.7 x 10^{-2} g/min/hole, Number of Layers: 2, DCD 15 cm, Take Up Speed: 20 '/min)

As was mentioned in our earlier discussion, with increasing attenuating air pressure the fraction of smaller fibers increases. An increase in the attenuating air pressure results in an increase in the velocity of the forming air and hence, an increase in the drag force exerted on the fiber. This leads to the formation of fine fibers. Finer fibers produced arrange themselves closer together and hence finer pores are formed in the web. Figure 19 shows the pore size distribution and the filtration efficiency of the webs produced at different attenuating air pressures. Complementing the pore size distribution, the filtration efficiency increases with increasing attenuating air pressure. A higher percentage of finer pores increase the filtration efficiency of the web [1, 4, 5].

Take-Up Speed and Through Put

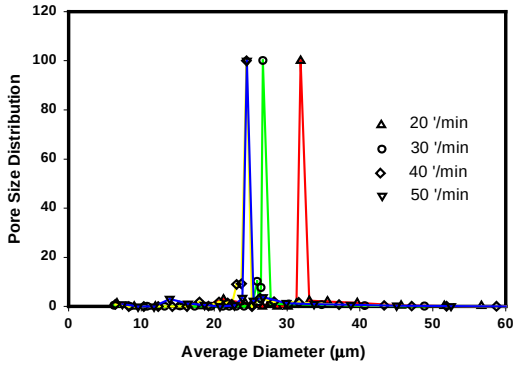

(a)

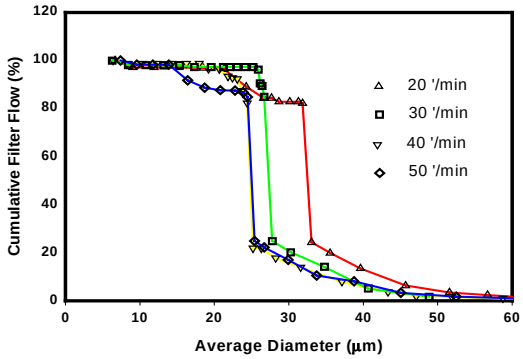

(b)

Figures 20 a & b. Pore Size Distribution and Cumulative Filter Flow(%) for MB PP Fabrics for variation in the web Take up Speed (Throughput : 3.7 x 10^{-2} g/min/hole, Number of Layers: 2, DCDC: 15 cm, Air Pressure: 1.4 bar)

As has been mentioned in the earlier discussions, increase in the take up speed of the web decreases the basis weight of the web. The increase in take up speed also increases the fiber orientation in the machine direction. The increase in the orientation in the machine direction and the decrease in basis weight due to increase in the take up speed decreases the average pore size and forms a narrower distribution, as also reported by Bhatia [4]. As is shown in Figure 20, the increase in take up speed decreases the pore size and increases the filtration efficiency of the web. But, at the current throughput rate, basis weight and

attenuating air pressure there is no change in the pore size and filtration efficiency when the take up speed is changed from 40 ft/min to 50 ft/min.

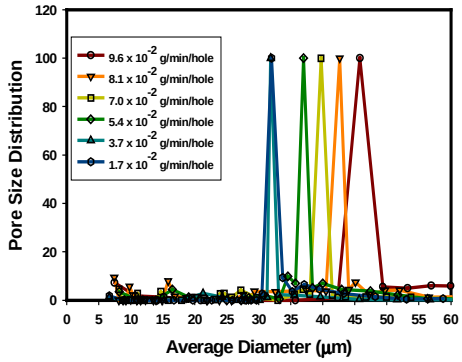

(a)

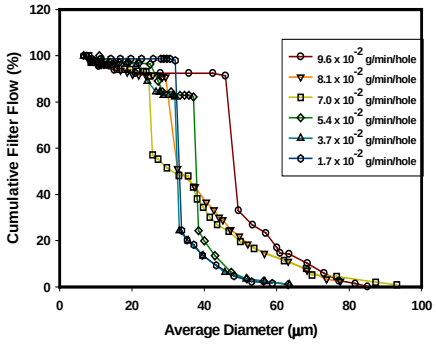

(b)

Figures 21 a & b. Pore Size Distribution and Cumulative Filter Flow (%) for MB PP Fabrics for variation in the Polymer Throughput (Take Up Speed: 20'/min., Number of Layers: 2, DCD: 15 cm, Air Pressure: 1.4 bar)

Figure 21 shows the pore size distribution and filtration efficiency of the webs for different throughput levels. Similar to the influence of through put on the diameter distribution of the fibers in the web [8], the average diameter of the pore size of the web decreases with the decrease in the through put through the meltblowing system. The diameter distribution range decreases. The filtration efficiency of the webs increases with the decrease in the average diameter of the pore size.

4. CONCLUSIONS

A novel 3D fiberweb manufacturing technology has been successfully developed. This Robotic Fiber Assembly & Control System (RFACS) can be implemented for production of seamless 3D meltblown nonwoven fabric structures. The set-up developed here allows for arbitrary positioning of the melt-blowing die in an initial reference frame to an arbitrary collecting surface without difficulty and accuracy of 1/10 of a millimeter.

Experiments have demonstrated that rotational motion of a mold needs to be controlled according to its shape (curvature, etc.), when uniform basis-weight distribution is required. Various motion correction models (i.e. linear and nonlinear) may be successfully employed to some extent. Relative movement and orientation of die and collecting surface must be considered carefully to achieve desirable results. For the case of fiber deposition on a mold, it is desirable to have the center of the tool carrying die aligned normal to the surface of the mold. Such an orientation allows for more uniform fiber application to the mold surface and results in a 4%-10% improvement in basis-weight uniformity. Implementation of a rule-base control algorithm that compensates for the mold position and speed as well as tool position was successfully done. The approach improves the basis-weight uniformity and significantly simplified the robot programming operation.

Fiber ODF is shown to be a useful parameter for detailed analysis of changes taking place in meltblown nonwoven structures. Changes induced in structures by variation of process parameters were appropriately related to respective changes observed in the fabric's ODF.

Changes in fabric take-up speed, die-to-collector-distance, fiber-stream approach-angle, polymer throughput rates, and attenuating air-pressures were shown to significantly affect fiber ODF in webs. Generally all fiber ODFs exhibited a bell-shaped pattern, with the highest frequency of orientation in the vicinity of MD. Changes in fiber-stream approach-angles were demonstrated to affect respective changes in fiber orientation distribution to the highest extent. For a change in fiber-stream approach-angle from normal (90°) to 36°, a 60 % increase in fiber alignment along the machine direction was shown.

Fiber diameter distributions were shown to correlate well to processing conditions employed in meltblowing of polypropylene resin. Fiber diameters were demonstrated to reduce with reductions in throughput rate, and increases in

attenuating air pressures and die temperatures. Air temperatures in the range studied, below 210 ºC at the die-orifice exit, were shown to not affect fiber diameter distributions. Good agreement for all results was also found to average fiber diameter data observed in published literature.

The pore size distribution and the filtration efficiency of the melt blown polypropylene webs were characterized. The effect of the process variables on the average pore size distribution was investigated. The changes in the average pore diameter were related to the diameter changes that take place in the fibers formed and their orientation distribution. The change in die-to-collector-distance, number of layers, attenuating air pressure, polymer throughput rates, and web take up speeds were shown to significantly affect the average pore size and the filtration efficiency of the webs formed. In the case of die to collector distance, the least pore size and the best filtration efficiency was formed at a distance of 15 cm. as the temperature of the attenuating air is dropped to around temperature beyond the 15 cm. This does not allow further changes in the internal structure of the fiber and also effects the consolidation of the fiber web on the collecting surface. The increase in attenuating air pressure from 0.7 bar to 2.8 bar reduces the average predominant pore size by 60%, while when the take up speed is increased from 20'/min to 50'/min, the average pore size reduces by 33%.

ACKNOWLEDGEMENTS

This research was supported in part by an ARO-MURI grant from the Army Research Office, and in part by support from the Nonwovens Cooperative Research Center, North Carolina State University. We gratefully acknowledge their generous support of this project.

REFERENCES

1. Allen,T., "Particle Size Measurement", 4th Ed., Chapman and Hall, New York, 1990.
2. Bansal, Vishal, R. L. Shambaugh, On-line Determination of Diameter and Temperature during Melt Blowing of Polypropylene, *Ind. Eng. Chem. Res.* **37**, 1799-1806 (1998).
3. Bergmann, L., "Microfiber And Electrostatically Charged Nonwovens in Filtration", *Nonwovens Industry* 22, (2), 28-34 (1991).
4. Bhatia, S. K., and Smith, J.L., "Geotextile Characterisation and Pore Size Distribution: Part I. A Review of Manufacturing Processes", *Geosynthetics International*, **3** (1), 85-105, 1996.
5. Bhatia, S. K., Smith, J. L., and Christopher, B. R., "Geotextile Characterisation and Pore Size Distribution: Part III. Comparison of Methods and Application to Design", *Geosynthetics International*, **3** (3), 301 – 328, 1996.
6. Chhabra, Rajeev, S, R. L. Shambaugh, Experimental Measurements of Fiber Threadline Vibrations in the Melt-Blowing Process, *Ind. Eng. Chem. Res.* **35**, 45366-4374 (1996).
7. Eian, G., "Durable Melt-Blown Fibrous Sheet Material, U.S. patent 4,681,801, 1987.
8. Farer, Raoul., Formation of 3D Meltblown Structures Using Robotic Control of Fiber Deposition, Doctoral Thesis, NCSU, Raleigh, NC, 1999.
9. Hearle, J. W. S., and Sultan, M. A. I., A Study of Needled Fabrics, Part IV, *J. Textile Inst.* **59**, 161 (1968).
10. Hearle, J.W. S., and Stevenson, P.J., Nonwoven Fabric Studies, Part III: The Anisotropy of Nonwoven Fabrics, *Textile Res. J.* **34**, 3 (1964).
11. Huang, X. C., and Breese, R. R., Characterizing Nonwoven Webs Using Image AnalysisTechniques, Part I: Pore Analysis in Thin Webs, *INDA J. Nonwovens Res.* **5** (2), 14 (1983).
12. Insley, T., "Sorbent Sheet Material", European patent application 0 156 649 A2, 1985.
13. Matsuoka, T., Takabatake, J., Inoue, Y., and Takahashi, H., Prediction of Fiber Orientation in Injection Molded Parts of Short-Fiber Reinforced Thermoplastics, *Polym. Eng. Sci.* **30**, 16, 957 (1990).
14. Petterson, D. R., Doctoral thesis, M.I.T., Cambridge, MA, 1958.
15. Pourdeyhimi, B., Ramanathan, R., Measuring Fiber Orientation in Nonwovens, Part I; Simulation, *Textile Res. J.* **66** (11), 713-722 (1996).

16. Rao, Rajiv. S, R. L. Shambaugh, Vibration and Stability in the Melt Blowing Process, *Ind. Eng.Chem. Res.* **32**, 3100-3111 (1993).

17. Schwarz, E. C. A., "Apparatus and Process for Melt-Blowing a Fiber forming Thermoplastic and Product Produced Thereby", U.S. Patent 4,380570, 1983.

18. Tate, Brian D., R. L. Shambaugh, Modified Dual Rectangular Jets for Fiber Production, *Ind. Eng. Chem. Res.* **37**, 3772-3779 (1998).

19. Uyttendale, Marc A. J., R. L. Shambaugh, The Flow Field of Annular Jets at Moderate Reynolds Numbers, *Ind. Eng. Chem. Res.* **28**, 1735-1740 (1989).

20. Uyttendale, Marc A. J., R. L. Shambaugh, Melt Blowing: General Equation Development and Experimental Verification, *AIChE Journal.* **36**, 175-186 (199

21. Veerabadran, K. Studies on Uniformity of Fiberweb Basis Weight and Structure, Doctoral Thesis, NCSU, Raleigh, NC, 1994.

22. Velu, Yogeshwar., Ghosh, Tushar., and Seyam., Abdelfattah., "Formation of Melt-Blowing Shaped/Molded Fabric Structures, Part II: Influence of Process Parameters on Pore Size Distribution" , Submitted for publication to Textile Research Journal.

23. Wadsworth, L., and Fagan, J., "Melt blown processing and Characterisation of Fluoropolymer Resins", *INDA J. Nonwovens Res*, **4** (4), 27 – 31.

24. Wadsworth, L. C., "Novel Melt Blown Research Findings", Nonwovens Industry, 17, (11), 44-51, 1986.

25. Wisneski, T. J., and Morman, M. T., "Polyolefin Containing Extrudable Compositions and Methods for their Formation into Elastomeric Products Including Microfibers", U.S. patent 4,663,220, 1987.

26. Xu, B., Measurement of Pore Characteristics in Nonwoven Fabrics Using Image Analysis, *Clothing and Textile Research Journal*., **14**, 81 – 88, 1996.

AUTHORS' INFORMATION

Yogeshwar Velu, Raoul Farer, Tushar Ghosh, Abdelfattah Seyam
College of Textiles
North Carolina State University
Raleigh, NC 27695, USA
Telephone: (919) 515-6568
FAX: (919) 515-3733